Baryon Stopping and Charged Particle Distributions in Central Pb + Pb Collisions at 158 GeV per Nucleon

H. Appelshäuser,[7,*] J. Bächler,[5] S. J. Bailey,[16] L. S. Barnby,[3] J. Bartke,[6] R. A. Barton,[3] H. Białkowska,[14] A. Billmeier,[10] C. O. Blyth,[3] R. Bock,[7] B. Boimska,[14] C. Bormann,[10] F. P. Brady,[8] R. Brockmann,[7,†] R. Brun,[5] P. Bunčić,[5,10] H. L. Caines,[3] D. Cebra,[8] G. E. Cooper,[2] J. G. Cramer,[16] P. Csato,[4] J. Dunn,[8] V. Eckardt,[13] F. Eckhardt,[12] M. I. Ferguson,[5] H. G. Fischer,[5] D. Flierl,[10] Z. Fodor,[4] P. Foka,[10] P. Freund,[13] V. Friese,[12] M. Fuchs,[10] F. Gabler,[10] J. Gal,[4] R. Ganz,[13] M. Gaździcki,[10] W. Geist,[13] E. Gładysz,[6] J. Grebieszkow,[15] J. Günther,[10] J. W. Harris,[17] S. Hegyi,[4] T. Henkel,[12] L. A. Hill,[3] I. Huang,[2,8] H. Hümmler,[10,‡] G. Igo,[11] D. Irmscher,[2,7] P. Jacobs,[2] P. G. Jones,[3] K. Kadija,[18,13] V. I. Kolesnikov,[9] M. Kowalski,[6] B. Lasiuk,[11,17] P. Lévai,[4] A. I. Malakhov,[9] S. Margetis,[2,§] C. Markert,[7] G. L. Melkumov,[9] A. Mock,[13] J. Molnár,[4] J. M. Nelson,[3] M. Oldenburg,[10] G. Odyniec,[2] G. Palla,[4] A. D. Panagiotou,[1] A. Petridis,[1] A. Piper,[12] R. J. Porter,[2] A. M. Poskanzer,[2] S. Poziombka,[10] D. J. Prindle,[16] F. Pühlhofer,[12] J. G. Reid,[16] R. Renfordt,[10] W. Retyk,[15] H. G. Ritter,[2] D. Röhrich,[10] C. Roland,[7] G. Roland,[10] H. Rudolph,[2,10] A. Rybicki,[6] A. Sandoval,[7] H. Sann,[7] A. Yu. Semenov,[9] E. Schäfer,[13] D. Schmischke,[10] N. Schmitz,[13] S. Schönfelder,[13] P. Seyboth,[13] F. Sikler,[4] E. Skrzypczak,[15] G. T. A. Squier,[3] R. Stock,[10] H. Ströbele,[10] I. Szentpetery,[4] J. Sziklai,[4] M. Toy,[2,11] T. A. Trainor,[16] S. Trentalange,[11] T. Ullrich,[17] M. Vassiliou,[1] G. Vesztergombi,[4] D. Vranić,[5,18] F. Wang,[2] D. D. Weerasundara,[16] S. Wenig,[5] C. Whitten,[11] T. Wienold,[2,*] L. Wood,[8] N. Xu,[2] T. A. Yates,[3] J. Zimanyi,[4] X.-Z. Zhu,[16] and R. Zybert[3]

(NA49 Collaboration)

[1]*Department of Physics, University of Athens, Athens, Greece*
[2]*Lawrence Berkeley National Laboratory, University of California, Berkeley, California 94720*
[3]*Birmingham University, Birmingham, United Kingdom*
[4]*KFKI Research Institute for Particle and Nuclear Physics, Budapest, Hungary*
[5]*CERN, Geneva, Switzerland*
[6]*Institute of Nuclear Physics, Cracow, Poland*
[7]*Gesellschaft für Schwerionenforschung (GSI), Darmstadt, Germany*
[8]*University of California at Davis, Davis, California 95616*
[9]*Joint Institute for Nuclear Research, Dubna, Russia*
[10]*Fachbereich Physik der Universität, Frankfurt, Germany*
[11]*University of California at Los Angeles, Los Angeles, California 90095*
[12]*Fachbereich Physik der Universität, Marburg, Germany*
[13]*Max-Planck-Institut für Physik, Munich, Germany*
[14]*Institute for Nuclear Studies, Warsaw, Poland*
[15]*Institute for Experimental Physics, University of Warsaw, Warsaw, Poland*
[16]*Nuclear Physics Laboratory, University of Washington, Seattle, Washington 98195*
[17]*Yale University, New Haven, Connecticut 06520*
[18]*Rudjer Boskovic Institute, Zagreb, Croatia*
(Received 22 October 1998)

Net proton and negative hadron spectra for central Pb + Pb collisions at 158 GeV per nucleon at the CERN Super Proton Synchrotron were measured and compared to spectra from lighter systems. Net baryon distributions were derived from those of net protons. Stopping (rapidity shift with respect to the beam) and mean transverse momentum $\langle p_T \rangle$ of net baryons increase with system size. The rapidity density of negative hadrons scales with the number of participant nucleons for nuclear collisions, whereas their $\langle p_T \rangle$ is independent of system size. The $\langle p_T \rangle$ dependence upon particle mass and system size is consistent with larger transverse flow velocity at midrapidity for Pb + Pb compared to S + S central collisions. [S0031-9007(99)08704-9]

PACS numbers: 25.75.Dw, 25.75.Ld

Lattice QCD predicts that strongly interacting matter at an energy density greater than $1-2$ GeV/fm^3 attains a deconfined and approximately chirally restored state known as the quark-gluon plasma (for an overview, see [1]). This state of matter existed in the early Universe, and it may influence the dynamics of rotating neutron stars [2]. The collision of nuclei at ultrarelativistic energies offers the possibility in the laboratory of creating strongly interacting matter at sufficiently high energy density to form a quark-gluon plasma [3]. Hadronic spectra from these reactions reflect the dynamics of the hot and dense zone formed in the collision. The baryon density, established

early in the reaction, is an important factor governing the evolution of the system [4]. Comparison of model predictions with measured rapidity and transverse momentum distributions and correlation functions constrains the possible dynamical scenarios of the reaction [5], such as those for longitudinal and transverse flow [6]. In addition, the mechanism by which the incoming nucleons lose momentum during the collision (baryon stopping [7]) is an important theoretical problem [8–10], and the measurement of baryon stopping in heavy ion collisions provides essential data on this question.

In this Letter, we present measurements by the NA49 Collaboration of rapidity and transverse momentum distributions of participating baryons and negative hadrons over a large fraction of phase space for central Pb + Pb collisions at 158 GeV per nucleon ($\sqrt{s_{NN}} = 17.2$ GeV). Hadronic spectra from S + S collisions at 200 GeV per nucleon [11–13] and $N + N$ (nucleon-nucleon) collisions at 200 and 400 GeV [14,15] serve as important references, helping to identify effects that depart from those expected from the linear superposition of many $N + N$ collisions.

The NA49 apparatus is described in [16]. A beam of ^{208}Pb ions at 158 GeV per nucleon ($y_{lab} = 5.8$) from the CERN Super Proton Synchrotron (SPS) struck a 224 mg/cm^2 thick natural Pb target. The 5% most central collisions were selected by measurement of the forward-going energy in the phase space occupied by the projectile spectator nucleons. The reaction products passed through a dipole magnetic field, and tracks from charged particles used for this analysis were measured in two large Main Time Projection Chambers (MTPCs) placed downstream of the magnets on either side of the beam axis. Over 1000 tracks were measured in each event. Identification of protons utilized the specific ionization ($\langle dE/dx \rangle$) of the gas of the MTPC [17]. A relative $\langle dE/dx \rangle$ resolution of 6% was achieved.

The evolution of the incoming baryons (baryon stopping) was studied through measurement of the difference of the proton and antiproton distributions (net protons, denoted $p - \overline{p}$) to eliminate the effect of baryon-antibaryon pair production. Meson production was studied through the yield of negative hadrons (h^-), comprising primarily π^-, with an admixture of K^- and $\overline{p}$. 5×10^4 central events were used for the $p - \overline{p}$ analysis and 7×10^3 central events were used for the h^- analysis.

The net proton yield was determined by an identification technique designed to minimize the systematic errors over wide acceptance [18]. For each phase space bin (y, p_T), the distribution of $\langle dE/dx \rangle$ from negatively charged particles was subtracted from that of positively charged particles, resulting in a distribution that contained a peak with positive amplitude (more positive than negative tracks, principally due to the net proton yield), and a peak at higher $\langle dE/dx \rangle$ with negative amplitude (net pions). In order to extract the particle yields, Gaussian functions were fitted to the two extrema in each difference distribution. A correction to the net proton yield for the difference between K^+ and K^- yields, based upon NA49 data [19], was 15% at $y_{\rm cm} < 0$ and was negligible for $y_{\rm cm} > 1$. The negative hadron yield was determined from the yield of all tracks from negatively charged particles excluding electrons, identified via $\langle dE/dx \rangle$.

Corrections for detector acceptance and track reconstruction efficiency were calculated by embedding and reconstructing simulated tracks in real events [18]. The tracking efficiency was greater than 95% over most of the acceptance, falling below 80% in regions of high track density and near the edges of the acceptance. Yield as a function of rapidity was determined only for bins having acceptance to $p_T = 0$, with the exception of the two lowest rapidity bins for h^- where extrapolation was based upon the adjacent bin having full coverage. At high p_T, the acceptance was limited to the region in which detector effects were well understood in this analysis, extending at least to $p_T = 2.0$ GeV/c for all rapidity bins. Instrumental background due to secondary interactions with detector material was estimated to be 5% of the total measured yield, using a GEANT-based Monte Carlo simulation and the VENUS event generator [10], which reproduces transverse and forward energy distributions in central Pb + Pb collisions [3]. Excluding the decay corrections discussed below, the systematic errors of all rapidity distributions were less than 10%.

The measured yields contain contributions from the products of weak decays that were incorrectly reconstructed as primary vertex tracks. The background correction to the h^- yield due to the decay of K^0_S was estimated using NA49 data [19] to be 5% at midrapidity, decreasing strongly at higher rapidity. Background to the h^- yield due to Λ decay is less than 1%. The background correction to the $p - \overline{p}$ yield is due to the decays of Λ, $\overline{\Lambda}$, Σ^+, and $\overline{\Sigma}^-$ and was assessed using a GEANT-based simulation of the decay of Λ and $\overline{\Lambda}$ and reconstruction of their charged decay products. (Λ and $\overline{\Lambda}$ should be understood in this paper to include the contributions of Σ^0 or $\overline{\Sigma}^0$ as well as feeddown from weak decays, which are not distinguishable from primary Λ or $\overline{\Lambda}$ in this analysis.) To investigate the dependence of this correction on the phase space distribution of the decaying particles, three different shapes of rapidity distribution for $\Lambda - \overline{\Lambda}$ were used, based upon (i) predictions of the RQMD model [9] and (ii) the VENUS model [10] and (iii) a preliminary NA49 measurement [20]. In each case the $\Sigma^+ - \overline{\Sigma}^-$ yield was assumed to be 30% of the $\Lambda - \overline{\Lambda}$ yield [21] and to have the same rapidity distribution. Strangeness is not conserved if both the hyperon yields in (i) or (ii) and the measured kaon distribution are used. The hyperon yields in these cases were therefore scaled by the ratio of charged kaon yields in the data and the model, thereby imposing strangeness conservation. In order to compare corrections due to $\Lambda - \overline{\Lambda}$ distributions differing only in shape but not total yield, the distribution in (iii) was scaled so that the ratio of $\Lambda + \Sigma^0$ to charged kaon yield agreed with that from the models. The $p - \overline{p}$ distribution

corrected by other $\Lambda - \overline{\Lambda}$ distributions can be derived from the figure.

Figure 1, upper panel, shows the event normalized net proton yield as a function of rapidity for central Pb + Pb collisions, incorporating the three $\Lambda - \overline{\Lambda}$ corrections and corresponding $\Lambda - \overline{\Lambda}$ rapidity distributions. Also shown is the proton rapidity distribution for $p + p$ collisions at 400 GeV [15], which is qualitatively different. The comparison highlights the importance of multiple collisions to baryon stopping in nuclear collisions.

To determine the net baryon $(B - \overline{B})$ rapidity distribution, the contribution of the remaining net baryons, in addition to $p - \overline{p}$ and $\Lambda - \overline{\Lambda}$, must be estimated. Model calculations [9,10] indicate that the rapidity distribution of net neutrons follows that of net protons over most of phase space, with a 7% larger yield. The contributions of $\Sigma^+ - \overline{\Sigma}^-$ and $\Sigma^- - \overline{\Sigma}^+$ were accounted for by assuming the same rapidity distributions as $\Lambda - \overline{\Lambda}$ and scaling the $\Lambda - \overline{\Lambda}$ distribution by an empirical factor 1.6 ± 0.1 derived from hadronic reactions [21]. Multistrange baryons contribute less than 2% to $B - \overline{B}$ [22] and were not accounted for. The net baryon yield $B - \overline{B}$ was then calculated as

$$B - \overline{B} = (2.07 \pm 0.05)(p - \overline{p}) + (1.6 \pm 0.1)(\Lambda - \overline{\Lambda}). \quad (1)$$

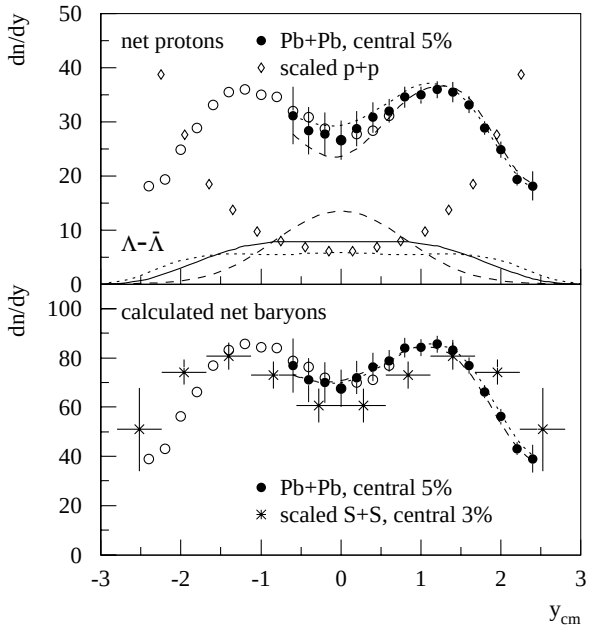

FIG. 1. Upper panel: Normalized rapidity distributions of $p - \overline{p}$ for Pb + Pb collisions incorporating correction (i) (open circles are data reflected about $y_{cm} = 0$; errors not shown). Lines show variation in data using corrections (ii) (dotted) and (iii) (dashed). Also shown are corresponding $\Lambda - \overline{\Lambda}$ rapidity distributions [(i) solid; (ii) dotted; (iii) dashed], and the scaled proton distribution for $p + p$ collisions. Lower panel: Normalized rapidity distributions of $B - \overline{B}$ from Eq. (1) for Pb + Pb incorporating correction (i), and scaled $B - \overline{B}$ for S + S. Lines correspond to corrections (ii) (dotted) and (iii) (dashed).

Figure 1, lower panel, shows the $B - \overline{B}$ rapidity distribution for Pb + Pb. The data points and errors are for $\Lambda - \overline{\Lambda}$ correction (i). The variation in $B - \overline{B}$ due to the use of different $\Lambda - \overline{\Lambda}$ corrections is smaller than that due to other sources of systematic error. The $B - \overline{B}$ yield is less sensitive than the $p - \overline{p}$ yield to the assumed $\Lambda - \overline{\Lambda}$ distribution, because the $\Lambda - \overline{\Lambda}$ distribution is removed from the measured $p - \overline{p}$ distribution by the decay correction but added again in Eq. (1) to calculate $B - \overline{B}$, with the two contributions approximately canceling. Conclusions on baryon stopping are therefore based upon the net baryon rather than net proton rapidity distribution. Also shown in Fig. 1, lower panel, is the $B - \overline{B}$ rapidity distribution for the 3% most central S + S collisions at 200 GeV per nucleon [12], using a coefficient of 2.0 for $p - \overline{p}$ in Eq. (1) and with integral normalized to the number of nucleon participants in Pb + Pb. Within $|y_{cm}| < 2.5$, there are 352 ± 12 participant baryons for Pb + Pb and 52 ± 3 for S + S central collisions [12].

The $B - \overline{B}$ rapidity distribution is narrower for Pb + Pb than for S + S collisions, indicating increased baryon stopping for Pb + Pb collisions. (In the c.m. frame, $y_{beam} = 2.9$ for Pb + Pb and 3.0 for S + S.) The median rapidity shift of the leading nucleon with respect to the beam in high energy p + Pb collision is 2–2.5 units [23]. Because of the symmetry of the nuclear reactions studied in this work, distributions of target and projectile nucleon rapidity shifts in full phase space cannot be determined separately, limiting the magnitude of a calculated rapidity shift even in the case of large baryon stopping. The mean rapidity shift relative to y_{beam} for participant baryons within $0 < y_{cm} < 2.5$ is $\langle \Delta y \rangle = -1.76 \pm 0.05$ for Pb + Pb and $\langle \Delta y \rangle = -1.63 \pm 0.16$ for S + S collisions.

Figure 2 shows the event normalized rapidity distribution (assuming pion mass) of h^- in central Pb + Pb and S + S [12] collisions, and isoscalar inelastic $N + N$ [14] collisions. An independent analysis of Pb + Pb collisions using the NA49 Vertex TPCs found a distribution consistent with these data [24]. The S + S and $N + N$ distributions were scaled relative to that for Pb + Pb by the ratio of the number of participant nucleons and a factor of 0.96 to account for the energy dependence of average multiplicities measured in hadronic collisions [25]. No correction for the net isospin difference between Pb + Pb and the other systems was applied. Under the assumption that the net isospin in the final state of a Pb + Pb collision is carried entirely by mesons, the additional scaling factor needed for comparison of the S + S and $N + N$ distributions to that of Pb + Pb is 1.12.

The enhancement of meson yield at midrapidity for nuclear collisions relative to $N + N$ collisions has been noted previously [11]. Taking into account the net isospin difference, the agreement between the Pb + Pb and scaled S + S distributions is striking. This scaling of the yield of produced particles with number of participants, first observed in $p + A$ collisions [23], is also observed

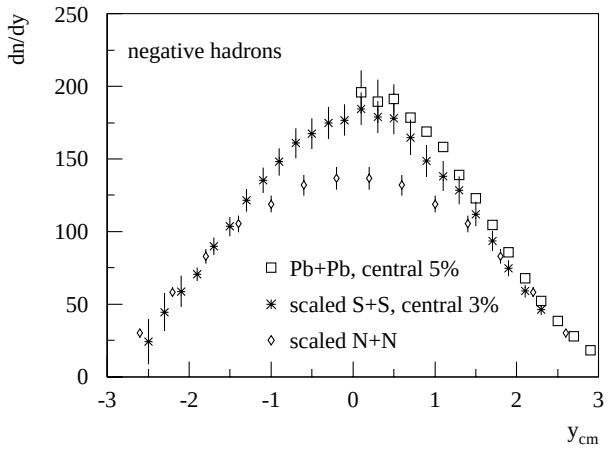

FIG. 2. Normalized rapidity distributions of h^- for central Pb + Pb collisions, and scaled central S + S and isoscalar inelastic $N + N$ collisions.

in the collision of very heavy ions. Extrapolation of the h^- yield to full phase space was performed by taking into account the asymmetry in the h^- rapidity distribution (assuming pion mass) due to the contribution of K^- [19], resulting in an estimated total h^- yield of 695 ± 30 particles. The number of h^- per participant nucleon pair, not adjusted for isospin, is 4.0 ± 0.2 for Pb + Pb collisions, compared to 3.6 ± 0.2 for S + S collisions and 3.22 ± 0.06 for isoscalar $N + N$ collisions [14].

Figure 3, upper panel, shows transverse mass spectra ($m_T = \sqrt{m^2 + p_T{}^2}$) near midrapidity for h^- and $p - \overline{p}$ for central Pb + Pb collisions. NA49 has previously reported the fit of an expanding hadronic source model [26] to midrapidity h^- and deuteron m_T spectra and h^- correlation functions [6], giving a freeze-out temperature of $T = (120 \pm 12)$ MeV and transverse expansion velocity $\beta_\perp = (0.55 \pm 0.12)$. Figure 3, upper panel, shows the fit of this model with fixed $\beta_\perp = 0.55$ to the h^- and $p - \overline{p}$ spectra reported here. The resulting freeze-out temperatures are $T = (126 \pm 2)$ MeV for h^- and $T = (118 \pm 5)$ MeV for $p - \overline{p}$.

Figure 3, lower panel, shows the rapidity dependence of $\langle p_T \rangle$ calculated within $0 < p_T < 2.5$ GeV. For $p - \overline{p}$ for central Pb + Pb collisions, $\langle p_T \rangle = (825 \pm 37)$ MeV at $y_{cm} = 0$ and (600 ± 17) MeV at $y_{cm} = 2.4$, compared to the rapidity-averaged value $\langle p_T \rangle = (622 \pm 26)$ MeV for central S + S collisions [11]. For h^- for central Pb + Pb collisions, $\langle p_T \rangle = (385 \pm 18)$ MeV at $y_{cm} = 0$, compatible with (377 ± 4) MeV for central S + S collisions [12]. (In considering $\langle p_T \rangle$ for h^- at high rapidity, note that the kinematic limit for pions for $N + N$ collisions at 158 GeV falls below $p_T = 1$ GeV near beam rapidity.)

A similar characterization of p_T distributions results from fitting $1/m_T dn/dm_T$ with a function $A \exp(-m_T/T)$. A fit within $0 < m_T - m_0 < 0.8$ GeV to the $p - \overline{p}$ data near midrapidity for central Pb + Pb collisions yielded $T = (308 \pm 15)$ [NA44 reported (289 ± 7) MeV for protons [13]]. NA35 found rapidity-averaged $T = (235 \pm 9)$ MeV for central S + S collisions [12]. The increase in T and $\langle p_T \rangle$ with particle mass is consistent with a larger transverse radial flow velocity at midrapidity in Pb + Pb than S + S collisions [6,13].

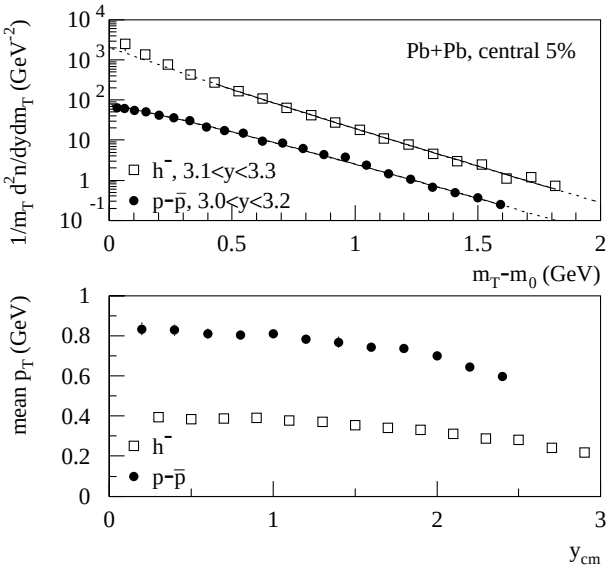

FIG. 3. Spectra for central Pb + Pb collisions. Upper panel: Transverse mass spectra near $y_{cm} = 0$. Solid lines indicate fits discussed in text; dotted lines are extrapolations of fit function. Lower panel: Rapidity dependence of $\langle p_T \rangle$ for h^- and $p - \overline{p}$.

In summary, baryon stopping for central collisions at ultrarelativistic energies increases with system size. The integrated yield and rapidity density of negative hadrons exhibit scaling with the number of participant nucleons for nuclear collisions, and a small enhancement with respect to $N + N$ collisions. At midrapidity, a large increase is observed in $\langle p_T \rangle$ for the stopped baryons in Pb + Pb relative to S + S collisions, with no significant increase in $\langle p_T \rangle$ for negative hadrons. The increase in $\langle p_T \rangle$ with particle mass is consistent with an increase in transverse radial flow velocity for heavier colliding systems.

This work was supported by the Director, Office of Energy Research, Division of Nuclear Physics of the Office of High Energy and Nuclear Physics of the U.S. Department of Energy under Contracts No. DE-AC03-76SF00098 and No. DE-FG02-91ER40609, the U.S. National Science Foundation, the Bundesministerium für Bildung und Forschung, Germany, the Alexander von Humboldt Foundation, the U.K. Engineering and Physical Sciences Research Council, the Polish State Committee for Scientific Research (2 P03B 02615 and 2 P03B 9913), the EC Marie Curie Foundation, and the Polish-Germany Foundation.

*Present address: Physikalisches Institut, Universitaet Heidelberg, Heidelberg, Germany.
†Deceased.
‡Present address: Max-Planck-Institut für Physik, Munich, Germany.
§Present address: Kent State University, Kent, OH 44242.

[1] *Proceedings of Quark Matter '96*, edited by P. Braun-Munzinger *et al.* [Nucl. Phys. **A610** (1996)].
[2] N. K. Glendenning, S. Pei, and F. Weber, Phys. Rev. Lett. **79**, 1603 (1997).
[3] T. Alber *et al.*, Phys. Rev. Lett. **75**, 3814 (1995).
[4] P. Koch, J. Rafelski, and W. Greiner, Phys. Lett. **123B**, 151 (1983); K. S. Lee, M. J. Rhoades-Brown, and U. Heinz, Phys. Rev. C **37**, 1452 (1988).
[5] E. Schnedermann and U. Heinz, Phys. Rev. C **50**, 1675 (1994); S. Chapman, J. R. Nix, and U. Heinz, Phys. Rev. C **52**, 2694 (1995); S. Chapman and J. R. Nix, Phys. Rev. C **54**, 866 (1996); T. Csörgö, B. Lorstad, and J. Zimanyi, Phys. Lett. B **338**, 134 (1994); T. Csörgö, Phys. Lett. B **347**, 354 (1995).
[6] H. Appelshäuser *et al.*, Eur. Phys. J. C **2**, 661 (1998).
[7] W. Busza and A. S. Goldhaber, Phys. Lett. **139B**, 235 (1984).
[8] A. Capella and B. Z. Kopeliovich, Phys. Lett. B **381**, 325 (1996); D. Kharzeev, Phys. Lett. B **378**, 238 (1996); B. Andersson, G. Gustafson, and H. Pi, Z. Phys. C **57**, 485 (1993); M. Gyulassy, V. Topor Pop, and S. Vance, Heavy Ion Phys. **5**, 299 (1997); S. E. Vance, M. Gyulassy, and X. N. Wang, nucl-th/9806008 (to be published).
[9] H. Sorge, Phys. Rev. C **52**, 3291 (1995).
[10] K. Werner, Phys. Rep. **232**, 87 (1993).
[11] J. Bächler *et al.*, Phys. Rev. Lett. **72**, 1419 (1994).
[12] T. Alber *et al.*, Eur. Phys. J. C **2**, 643 (1998).
[13] I. G. Bearden *et al.*, Phys. Rev. Lett. **78**, 2080 (1997).
[14] M. Gaździcki and O. Hansen, Nucl. Phys. **A528**, 754 (1991).
[15] M. Aguilar-Benitez *et al.*, Z. Phys. C **50**, 405 (1991).
[16] S. Wenig *et al.*, Nucl. Instrum. Methods Phys. Res., Sect. A **409**, 100 (1998).
[17] B. Lasiuk *et al.*, Nucl. Instrum. Methods Phys. Res., Sect. A **409**, 402 (1998).
[18] M. Toy, Ph.D. thesis, UCLA, 1999.
[19] NA49 Collaboration (to be published).
[20] C. Bormann *et al.*, J. Phys. G **23**, 1817 (1997).
[21] A. Wróblewski, Acta Phys. Pol. B **16**, 379 (1985).
[22] E. Andersen *et al.*, Phys. Lett. B **433**, 209 (1998).
[23] W. Busza and R. Ledoux, Annu. Rev. Nucl. Part. Sci. **38**, 119 (1988).
[24] J. Günther, Ph.D. thesis, University of Frankfurt, 1997.
[25] M. Antinucci *et al.*, Lett. Nuova Cimento **6**, 121 (1973).
[26] S. Chapman, P. Scotto, and U. Heinz, Heavy Ion Phys. **1**, 1 (1995).